Retrieval of Dry-Snow Parameters From Microwave Radiometric Data Using a Dense-Medium Model and Genetic Algorithms

Marco Tedesco, *Member, IEEE*, and Edward J. Kim, *Senior Member, IEEE*

***Abstract*—A numerical technique based on genetic algorithms (GAs) is used to invert the equations of an electromagnetic model based on dense-medium radiative transfer theory (DMRT) to retrieve snow depth, mean grain size, and fractional volume from microwave brightness temperatures. In order to study the sensitivity of the GA to its parameters, the technique is initially tested on simulated microwave data with and without adding a random noise. A configuration of GA parameters is selected and used for the retrieval of snow parameters from both ground-based observations and brightness temperatures recorded by the Advanced Microwave Scanning Radiometer-EOS (AMSR-E). Retrieved snow parameters are then compared with those measured on ground. Although more investigation is required, results suggest that the proposed technique is able to retrieve snow parameters with good accuracy.**

***Index Terms*—Dense-medium radiative transfer theory (DMRT), genetic algorithms (GAs), microwave remote sensing, snow.**

I. Introduction

SNOW covers a large area of the Earth during the winter, and the knowledge of its extension and properties is useful for hydrological, meteorological, and climatological applications. Microwave remote sensing represents a useful tool for studying the snow distribution and its properties at large scale.

The retrieval of snow parameters from electromagnetic quantities implies the inversion of the relationships relating the parameters to observed microwave radiometric quantities. This problem is not straightforward, and it has been the subject of several studies during the past years (e.g., [1]–[8]).

Existing techniques for the retrieval of snow parameters can be classified as empirical, semiempirical, and theoretical ones. Empirical techniques are based on the relationships between measured radiometric data and observed snow parameters, which often are expressed in terms of linear regressions (e.g., [1]–[4]). These techniques offer the possibility of an easy inversion, but they might have local validity.

Manuscript received May 18, 2005; revised January 23, 2006.

M. Tedesco is with the Goddard Earth Science Technology Center, University of Maryland, Baltimore County, and also with National Aeronautics and Space Administration Goddard Space Flight Center, Greenbelt, MD 20771 USA (e-mail: mtedesco@umbc.edu).

E. J. Kim is with the Laboratory For Hydrospheric and Biospheric Processes, National Aeronautics and Space Administration Goddard Space Flight Center, Greenbelt, MD 20771 USA.

Digital Object Identifier 10.1109/TGRS.2006.872087

Semiempirical techniques are based on both theoretical models and experimental data [5], [6]. Here, some of the parameters in the radiative transfer equation are derived from measured quantities. Snow parameters can be retrieved by inverting the equations either numerically or analytically. In the latter case, the convergence of the solution may be driven by constraints given by ground data and/or by considerations from the observed scene (i.e., possible values). The range of validity of semiempirical techniques is wider than that one of the empirical ones, though some limitations still exist.

The techniques having the widest validity are those ones based on the inversion of theoretical models. However, it is not always possible to perform the inversion of such equations by means of analytical techniques because of the difficulties of inverting nonlinear integro-differential equations (e.g., radiative transfer equations). Therefore, numerical approaches, such as iterative techniques or artificial neural networks (ANNs) (i.e., [7] and [8]) are often used. In the case of iterative techniques (e.g., the Nelder–Mead simplex method [9]), the convergence of the algorithm is not always guaranteed, especially in a multidimensional space (when we are looking for more than one parameter concurrently). In addition, the solution in the iterative techniques is strongly dependent on the initial conditions. ANN techniques are based on the training of the network by means of simulated or measured data and have demonstrated good performance [7], [8]. ANNs are very useful for real-time applications as, once trained, these can provide very fast responses.

A numerical technique potentially suitable for the retrieval of snow parameters by means of the inversion of the radiative transfer equation is represented by the genetic algorithms (GAs). So far, no study has been conducted on the possibility of using GA for this purpose, and this is the aim of this paper. In the following, we evaluate the capabilities of GA to invert the equations of an electromagnetic model based on dense-medium radiative transfer theory (DMRT) to retrieve fractional volume, snow depth, and mean grain size.

GAs are numerical iterative procedures where a population of individuals is described by a finite string of symbols (genome) and encode a possible solution in a given problem space (in the case of snow, each chromosome is a vector containing the three values of the fractional volume, snow depth, and mean grain size). The latter is named the search space and comprises all possible solutions to the problem (e.g., all possible combinations of snow parameters). The solution is reached by an iterative procedure and genetically inspired operators (i.e., crossover between two parents and mutation).

Among the benefits of using GA with respect to other techniques, there is the fact that the initial guess is not a single set, as it happens in the majority of numerical techniques (e.g., Nelder–Mead), but it is made of the entire initial population, whose size is a user-defined option. Also, GA operators (such as the mutation or the crossover operators) prevent premature convergence to local solutions by creating heterogeneity in the search space.

The GA-based inversion technique is applied to both simulated and measured brightness temperatures. A configuration of GA parameters is selected from the analysis of the inversion of simulated brightness temperatures and it is then used for the retrieval of snow parameters from both ground-based and spaceborne brightness temperatures. Ground observations of brightness temperatures were collected during the Cold Land Processes Experiment-1 (CLPX-1). Snow parameters collected on the ground in conjunction with radiometric measurements [10]–[12] are used to evaluate the retrieval performance. Also, brightness temperatures recorded by the Advanced Microwave Scanning Radiometer-EOS (AMSR-E) during the season 2003–2004, over Russia, are used. In this case, the validation set is provided by measurements performed by an automatic weather station.

The paper is divided as follows. In Section I, the GA-based technique and the electromagnetic model are presented. We report in Section II a discussion on the parameters of both GA and snow. Section III is devoted to the presentation of results and discussion. Finally, in Section IV, we report the conclusions and describe future work.

II. GAs and the DMRT Electromagnetic Model

In this section, we give a brief overview of GAs, primarily to introduce the terminology needed in later sections. Then, we report the base of the DMRT-based electromagnetic model used in this study together with a sensitivity analysis.

A. GAs

GAs are iterative procedures in which a population of individuals encode a possible solution to a given problem. They are based on Darwin's theory of evolution where problems are solved by an evolutionary process resulting in a best solution (survivor). Evolutionary computing was introduced in the 1960s by Rechenberg [13]–[16]. From Rechenberg's work, John Holland invented and developed GAs [e.g., [16]].

The GA begins with an initial population of individuals that are decoded and evaluated according to a fitness function, which numerically encodes the performance of each individual. Individuals with highest values of fitness are selected to continue to the successive iteration. Selection procedures alone cannot generate new individuals into the population, meaning that it is not possible to find solutions different from those ones generated in the initial population. It is therefore necessary to introduce new operators such as the crossover and mutation operators. The former is applied to two selected individuals (parents), by exchanging parts of their genomes to form two new individuals (offspring). The crossover operator is controlled by the probability that chromosomes are recombined and it is a user-defined parameter, usually set to a high value (95% for all cases reported in this study). The probability that a mutation occurs is another user-controlled option, and it is usually set to a low value (5% in our study), so that good chromosomes are not destroyed. A mutation simply changes the value for a particular gene. Fig. 1 shows a flux diagram for the GA.

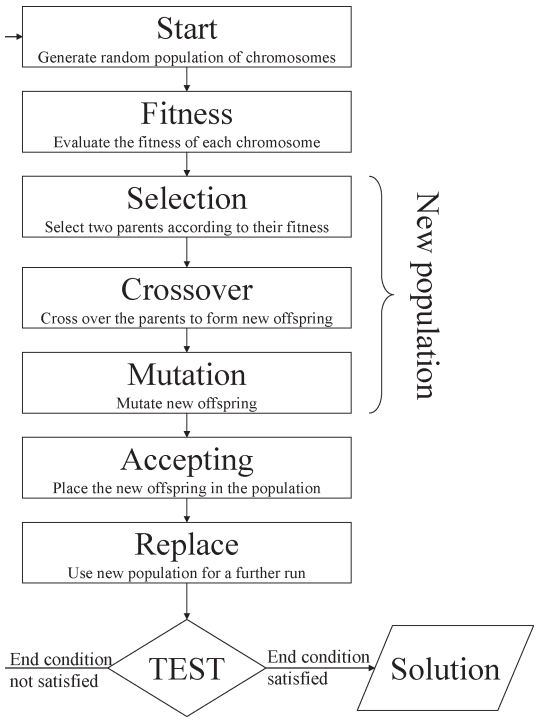

Fig. 1. Flux diagram for the GA.

B. Electromagnetic Model and Sensitivity Analysis

The equations of an electromagnetic model based on DMRT under the quasi-crystalline approximation with coherent potential (QCA-CP) [17], [18] are inverted to retrieve dry-snow parameters. A dense-medium-based model is fundamental to describe propagation and scattering in dry snow, where the assumption of independent scattering is not valid and dependent scattering must be considered. In the model, the effective propagation constant and albedo are computed under the Percus–Yevick (P–Y) approximation. The snowpack is modeled as a slab of densely distributed spherical particles with radius a and permittivity ε_i, embedded in a background medium of permittivity ε_b and lying above a soil having permittivity ε_g. The expressions for the effective propagation constant K and albedo ω can be found in [17] and [18]. The DMRT equations assume the same form as the classical radiative transfer equations and can be solved by using Gaussian quadrature and eigenvalues and eigenvectors analysis. The unknown coefficients derived from eigenvector analysis can be calculated by means of boundary conditions [18].

In order to perform the retrieval, it is important that the radiometric quantities involved are sensitive to snow parameters. Sensitivity analyses have been conducted and they

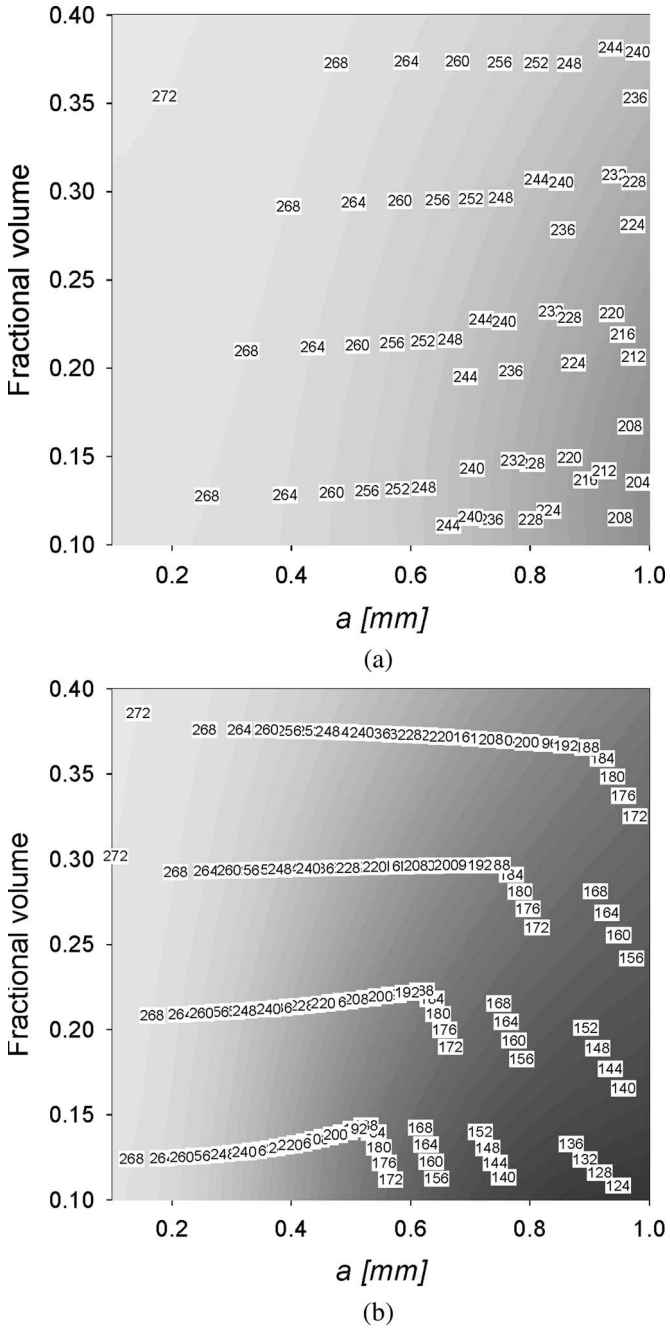

Fig. 2. Sensitivity analysis of the electromagnetic model. Brightness temperature (vertical polarization) as a function radius and fractional volume at (a) 19 and (b) 37 GHz.

can be found in the literature [17]–[19]. A sensitivity analysis involving two parameters is conducted using the DMRT model in this study. A strong sensitivity is shown by the 37-GHz channel to the mean particle size with the sensitivity decreasing as the frequency decreases. Brightness temperatures show less sensitivity to the fractional volume than to mean particle size, at both frequencies. Finally, the parameter showing the weakest sensitivity is the snow depth, meaning that large changes in the snow depth may only result in relatively small variations of brightness temperatures. As an example, Fig. 2 shows brightness temperatures at vertical polarization as a function of radius and fractional volume at 19 (a) and 37 (b) GHz.

III. Parameter Values

In this section, we discuss the values of GA parameters and report the results of a sensitivity analysis. We also discuss the range in which the snow parameters are allowed to range.

A. Parameters in the GA

The use of GA fundamentally requires the choice of six parameters: 1) chromosomes representation; 2) selection function; 3) genetic operators and reproduction function; 4) evaluation function; 5) initial population; and 6) termination criterion. In this section, we study how the choice of the values for the size of initial population, the convergence error, and of the number of initial iterations can influence the algorithm performance. To this aim, we simulated a set of brightness temperatures and applied the GA technique several times, changing only the population size, the number of initial iterations, and the error convergence. The chromosome representation, selection function, genetic operators, reproduction, and evaluation functions are kept fixed during this testing. In the following, we describe both the fixed and variable parameters of the GA.

1) Fixed Parameters:

a) Chromosome representation: The chromosome representation describes each individual in the population of interest by means of an alphabet. The alphabets used to describe each individual could consist of binary digits, floating-point numbers, integers, symbols, etc. In Holland's original design, the alphabet was limited to binary digits. Since then, problem representation has been the subject of many investigations and it has been shown that more natural representations are more efficient and produce better solutions [20]. Also, it has been demonstrated that good properties of GA do not stem from the use of bit strings [21], [22]. In [21], the author presents a new schema interpretation that overturns the theoretical suitability of the binary alphabet in favor of the high cardinal alphabets.

In this paper, we use a floating-point alphabet in which a chromosome is a vector of floating-point numbers. The precision is restricted to that of the computer where the algorithm is carried out. The size of the chromosomes is kept the same as the length of the vector, which is the solution to the problem (e.g., number of snow parameters to be retrieved), with each gene representing a variable of the problem. Note that the use of real parameters allows us to use large domains for the variables, which is difficult to achieve in binary implementations where increasing the domain would mean sacrificing precision, assuming a fixed length for the chromosomes.

b) Selection function: Several selection methods exist in the literature such as tournament selection, roulette wheel, and ranking methods [23]. In this paper, we use the tournament-selection method, in which each chromosome in the population competes for a position in the mating subset. The selection works as follows. Two chromosomes are drawn at random from the population, and the chromosome with the highest fitness score is placed in the mating subset; then, both chromosomes

are returned to the population and another tournament begins. This procedure continues until the mating subset is full. A main characteristic of this scheme is that the worst chromosome in the population will never be selected for inclusion in the mating subset. The maximum number of chromosomes in the tournament-selection method is set to ten. This choice is based on other studies conducted in [19].

c) Genetic operators: The choice of the representation for the individuals influences the choice of the genetic operators. Different crossover operators can be used in the case of the representation of individuals using a floating-point alphabet (e.g., simple crossover, arithmetic crossover, and heuristic crossover). In this study, we use the arithmetic crossover, which takes two parents (P1 and P2) and performs an interpolation along the line formed by the two parents. If $\underline{X}$ and $\underline{Y}$ are the two parents, then two offspring are produced by the arithmetic crossover as appears in (1), where r is a uniform random number between 0 and 1. The multi-nonuniform operator is used for the mutation where all parameters of the parent are changed on the basis of a nonuniform probability distribution [23], which allows the tuning to be produced in a suitable and fast way. The nonuniform mutation randomly selects one variable and sets it equal to a nonuniform random number as in (2), where a_i and b_i are, respectively, the lower and upper bounds, r_1 and r_2 are two uniform random numbers between 0 and 1, and $f(G) = (r_2(1 - G/G_{\max}))^b$, with G representing the current generation, $G_{\max}$ the maximum number of generations, and b is a shape parameter. The shape factor b is fixed to three [23].

$$\begin{aligned} \underline{X}' &= r\underline{X} + (1-r)\underline{Y} \\ \underline{Y}' &= (1-r)\underline{X} + r\underline{Y} \end{aligned} \tag{1}$$

$$x' = \begin{cases} x + (b_i - x) f(G) \rightarrow r_1 < 0.5 \\ x + (x + a_i) f(G) \rightarrow r_1 \geq 0.5 \\ x \rightarrow \text{otherwise.} \end{cases} \tag{2}$$

Let us report an example regarding the retrieval of one single snow parameter, such as mean grain size. Let the lower and upper bounds be $a_i = 0.1$ mm and $b_i = 2$ mm, the maximum number of generations $G_{\max} = 500$, the current generation $G = 100$, the shape parameter $b = 0.3$, $r_1 = r = 0.234$ and $r_2 = 0.675$, and $\underline{X} = 0.345$ mm and $\underline{Y} = 0.678$ mm. The results of the crossover operator are $\underline{X}' = 0.600$ mm and $\underline{Y}' = 0.422$ mm. The performances of the offspring are evaluated through the evaluation function and compared with those of the parents. Among the four (parents and offspring), the two individuals showing the best performances are selected for the next generation. In the case of the mutation operator, we have $f(G) = f(100) = 0.831$, $r_1 < 0.5$, implying $x' = 0.345 + (2 - 0.345) * 0.831 = 1.72$ mm. Note that the effects of the mutation operator on the individual decrease as the number of generations increase (e.g., for $G = 400$, $f(G) = 0.548$ and for $G = G_{\max}$ $f(G) = 0$).

d) Evaluation function: The evaluation function is represented by the root mean square error (rmse) between the brightness temperatures to be inverted (which will be named "target brightness temperatures" in the following) and the brightness temperatures obtained with the elements of the population.

2) Variable Parameters:

a) Initial population and population size: The population size dictates the number of chromosomes in the population. Larger population sizes increase the amount of variation present in the initial population at the expense of computation time. In our paper, we consider three values of population size having, respectively, 15 ($5 * N$, with $N = 3$ being the number of parameters to be retrieved), 30 ($10 * N$), and 60 ($20 * N$) individuals. Generally, a large population size is preferred to maintain diversity among the individuals, and hence allows better exploration of the solution space. An alternative to the use of a high number of individuals in the initial population is to keep high mutation rates and uniform crossover. However, this case is not examined in this paper. The number of initial iterations, being the number of iterations performed on the initial population, is also another parameter considered for the sensitivity analysis. In the cases here studied, this parameter could be 10 or 50 iterations.

b) Termination criterion: The algorithm stops either when the rmse between brightness temperatures retrieved by the GA algorithm and those to be inverted reaches a fixed value or a maximum number of iterations. We study the effect of changing the convergence-error value on the GA performance. Two values of error are considered: 0.1 and 10 K. The maximum number of iterations is fixed at 50 because we observe that no substantial improvement derives from using higher values.

B. Snow Parameters

In the case of the inversion of simulated brightness temperatures and ground-based measurements, the ranges of values in which snow parameters are allowed to range are the following: snow depth 0.1–1.5 m, particle size (diameter) 0.1–3 mm, fractional volume 0.1–0.4 (corresponding to a density ranging between 90 and 370 kg/m^3). Ice permittivity is computed according to Hufford [24] as a function of frequency and snow temperature. The remaining input parameters to the electromagnetic model are kept fixed as follows: snow temperature $T_{\text{snow}} = 269$ K, ground temperature $T_{\text{ground}} = 273$ K, ground permittivity $\varepsilon_{\text{ground}} = 4.5 + i0.1$. These values are the same as those used in the simulations to generate the simulated target temperatures. In addition, they are very close to the values obtained from field measurements for those cases when the technique is applied to experimental brightness temperatures [12]. The effects of roughness at the air/snow and snow/soil interfaces are neglected for simplicity, but will be considered in future studies.

In the case of the retrieval from space-borne data, also, the snow and air temperatures (which, for simplicity, were assumed to be the same) were allowed to range between 240 and 273 K. The soil temperature was fixed at 260 K. This is necessary if we want to take into account the seasonal variations of the soil and snow temperatures. All other parameters are kept with fixed.

IV. Results and Discussion

Before proceeding with the exposition of the results, we remind here that GA are stochastic procedures, meaning that

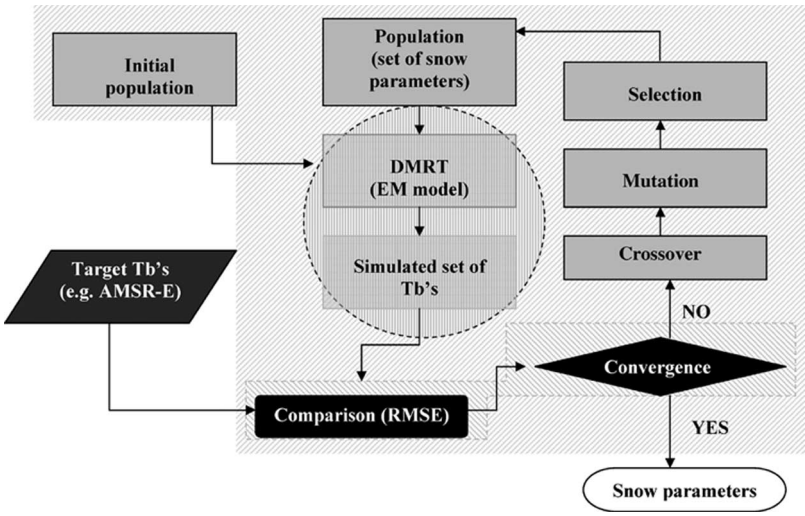

Fig. 3. Flux diagram of the GA-based inversion technique.

the solution can change even starting from the same population. Because of this, the results reported in the following are obtained as follows. Multiple runs (M) of the GA algorithm are performed for each set of unknown snow parameters, and the final solution is given by the mean of the M solutions showing an error lower than a fixed threshold. In this paper, the value of M was fixed to 50, and it was selected to guarantee enough number of solutions to average the results.

The link between the GA and the DMRT model is depicted in Fig. 3, where the flux diagram of the GA-based inversion technique is reported. For each set of brightness temperatures to be inverted, an initial population is generated and each element is evaluated by means of the rmse between the brightness temperatures obtained by means of the DMRT model driven by the elements of the population and the target brightness temperatures (e.g., AMSR-E brightness temperatures). If the termination criterion is satisfied, then the algorithm stops and the solution having the lowest rmse is selected. If the termination condition is not satisfied, then the existing population is subject to crossover, mutation, and selection to generate a new population, which is in turn used to generate a new set of brightness temperatures to be compared with the target brightness temperatures. The process is then iterated until the convergence (termination criterion) is satisfied.

The GA software used in this study is a modified version of the GA Optimization Toolbox (GAOT) for Matlab 5 by Houck *et al.* [23].

A. Application to Simulated Brightness Temperatures

In the following, we report the results of the inversion technique applied to simulated brightness temperatures with and without adding a random noise ranging between ± 5 K.

Noise-Free Simulated Brightness Temperatures: Table I summarizes the different combinations of GA parameters analyzed. In the cases A–D, the technique is applied to noise-free simulated brightness temperatures. In the cases D2–F, a random error of ± 5 K is added to the simulated brightness temperatures. The results obtained for the cases without added error (from A to D) are reported in Table II. In the example reported, the snow parameters used to generate the simulated brightness temperatures (and hence, to be retrieved) are: diameter $D = 2a = 1$ mm, fractional volume $f = 0.3$ and snow depth $d = 0.8$ m. In Table II, two results are reported for each parameter: The case named "initial selection" refers to the value obtained by using only the initial iterations. Results show that the parameter retrieved with the lowest error (between 1.2% and 3.6%) and standard deviation is the mean grain size. The values of fractional volume are retrieved with an error between 11% and 16%. The values of snow depth are retrieved with an error between 8.8% and 27.5%. The results also show that the choice of GA parameters does not strongly affect the retrieval of mean particle size or fractional volume. The retrieval of snow depth, however, does improve as the size of the initial population increases (cases C and D), mainly because of the increase in the diversity of the initial population.

TABLE I
TEST CONFIGURATIONS FOR THE GA-BASED TECHNIQUE

	A	B	C	D	D2	E	F
Population size	15	15	30	60	60	15	15
Init. iteration	10	50	10	10	10	10	10
Convergence it.	50	50	50	50	50	50	50
Conv. Error [K]	0.1	0.1	0.1	0.1	10	0.1	10
Added Random error [K]	0	0	0	0	±5	±5	±5

Noisy Simulated Brightness Temperatures: Results obtained when random noise (± 5 K) is added to the simulated brightness temperatures are reported in Table III. Reference values for snow parameters are the same as those used previously ($D = 2a = 1$ mm, $f = 0.3$, and $d = 0.8$ m). As it happened in the case of noise-free brightness temperatures, mean particle size shows a weak sensitivity to GA-parameter variations. Tables IV and V show the results obtained with the technique applied to different sets of snow parameters, using the F and D2 configurations. The case denoted with D2 was not initially considered, but it was suggested by the encouraging results obtained with the case D. The D2 configuration gives better results than the F configuration, but they both fail in case #2.

TABLE II
RESULTS FOR DIFFERENT GA CONFIGURATION PARAMETERS IN THE CASE OF BRIGHTNESS TEMPERATURES WITHOUT NOISE. EXPECTED VALUES ARE: $a = 0.5$ mm, $f = 0.3$, AND $d = 0.8$ m. MEAN ERROR REPRESENTS THE DIFFERENCE BETWEEN THE RETRIEVED AND EXPECTED VALUE (NEGATIVE ERROR MEANS UNDERESTIMATION, AND POSITIVE ERROR MEANS OVERESTIMATION)

	A				B				C				D			
	Mean value	**Std. Dev**	**Mean error**	**Relative perc. error [%]**	**Mean value**	**Std. Dev**	**Mean error**	**Relative perc. error [%]**	**Mean value**	**Std. Dev**	**Mean error**	**Relative perc. error [%]**	**Mean value**	**Std. Dev**	**Mean error**	**Relative perc. error [%]**
Radius [mm]																
Initial selection	0.511	0.1	0.011	2.2	0.512	0.107	0.012	2.4	0.493	0.08	-0.007	1.4	0.493	0.08	-0.007	1.4
Convergence value	0.506	0.07	0.006	1.2	0.487	0.069	-0.013	2.6	0.482	0.06	-0.018	3.6	0.491	0.08	-0.009	1.8
Fractional volume																
Initial selection	0.261	0.09	-0.039	13	0.242	0.09	-0.058	19.3	0.247	0.08	-0.053	17.6	0.266	0.08	-0.034	11.3
Convergence value	0.257	0.08	-0.043	14.3	0.253	0.06	-0.047	15.6	0.252	0.07	-0.048	16	0.267	0.08	-0.033	11
Depth [m]																
Initial selection	0.553	0.24	-0.247	30.87	0.565	0.288	-0.235	29.3	0.664	0.231	-0.136	17	0.724	0.213	-0.076	9.5
Convergence value	0.58	0.23	-0.242	27.5	0.645	0.211	-0.155	19.3	0.68	0.190	-0.12	15	0.721	0.199	-0.079	9.8

TABLE III
RESULTS FOR DIFFERENT GA CONFIGURATION PARAMETERS IN THE CASE OF NOISY BRIGHTNESS TEMPERATURES. EXPECTED VALUES ARE: $a = 0.5$ mm, $f = 0.3$, AND $d = 0.8$ m

	E		F	
Radius [mm]	**Mean**	**Std. dev**	**Mean**	**Std. dev**
Initial selection	0.511	0.102	0.509	0.09
Convergence value	0.515	0.094	0.511	0.09
Fractional volume				
Initial selection	0.264	0.09	0.251	0.09
Convergence value	0.27	0.08	0.257	0.08
Depth [m]				
Initial selection	0.636	0.243	0.566	0.267
Convergence value	0.63	0.238	0.593	0.263

TABLE IV
RESULTS OF THE GA ALGORITHM FOR DIFFERENT COMBINATIONS OF SNOW PARAMETERS USING CONFIGURATION F

	Case F	**Depth [m]**	**Fractional volume**	**Radius [mm]**
	Depth[m], Fractional volume, Radius [mm]			
1	0.8 0.35,0.3	0.503±0.237	0.242±0.08	0.644±0.09
2	0.2,0.2,0.5	0.566±0.244	0.242±0.07	0.222±0.06
3	0.6,0.3,0.6	0.534±0.254	0.27±0.09	0.616±0.11
4	0.5,0.3,0.8	0.64±0.267	0.257±0.09	0.51±0.09
5	0.8,0.38,0.8	0.53±0.272	0.281±0.09	0.745±0.11

TABLE V
RESULTS OF THE GA ALGORITHM FOR DIFFERENT COMBINATIONS OF SNOW PARAMETERS USING CONFIGURATION D2

	Case D2	**Depth [m]**	**Fractional volume**	**Radius [mm]**
	Depth[m], Fractional volume, Radius [mm]			
1	0.8,0.35,0.3	0.65±0.17	0.29±0.06	0.24±0.06
2	0.2,0.2,0.5	0.581±0.22	0.22±0.07	0.21±0.05
3	0.6,0.3,0.6	0.593±0.23	0.26±0.09	0.59±0.09
4	0.5,0.3,0.8	0.547±0.25	0.26±0.08	0.63±0.08
5	0.8,0.38,0.8	0.49±0.22	0.29±0.08	0.75±0.1

B. Application of the GA to Measured Brightness Temperatures

The configuration denoted as D2 is used in the following to extract snow parameters from measured brightness temperatures.

Ground Radiometric Data: Ground microwave radiometric data used in this study were collected by the University of Tokyo's ground-based microwave radiometer (GBMR-7) during the National Aeronautics and Space Administration (NASA) Cold Land Process Experiment (CLPX-1) in February 2003 [10]. During the experiment, measurements of snow properties were performed at least daily [25]. Snow parameters collected in the field are averaged along the vertical profile of the snowpack and compared with those retrieved using the GA-based technique applied to the GBMR-7 data. The values of snow parameters are averaged along the vertical profile as follows: The snowpack is divided in a number of layers, each of them 10 cm thick. For each layer, snow parameters were averaged by considering the extinction of the layers overlying the layer in object and, for each frequency, the average values were computed. Finally, the value reported in the table is obtained by averaging the values obtained at the two frequencies. Figs. 4 and 5 show the results obtained, respectively, for fractional volume and snow depth. In more detail, Fig. 4 shows the comparison between average values of measured fractional volume (black circles) versus retrieved fractional volume (white squares). For all dates, the retrieved values

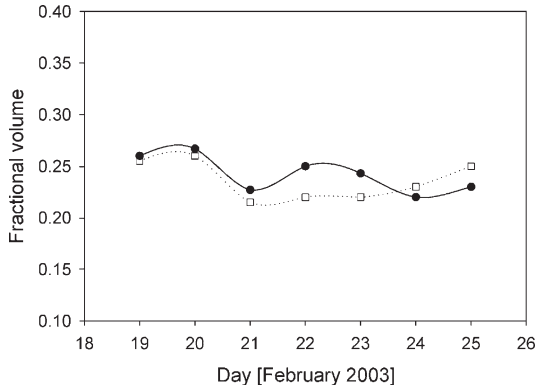

Fig. 4. Measured (squares) and retrieved (circles) fractional volume for the different dates of the CLPX-1 IOP3 period.

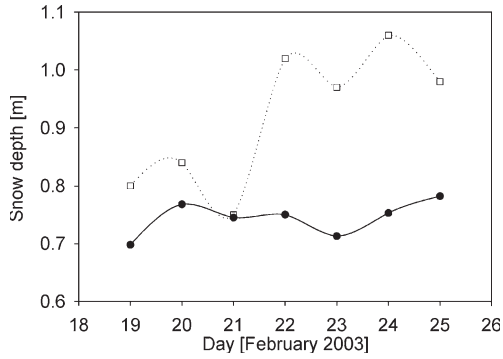

Fig. 5. Measured (squares) and retrieved (circles) snow depth for the different dates of the CLPX-1 IOP3 period.

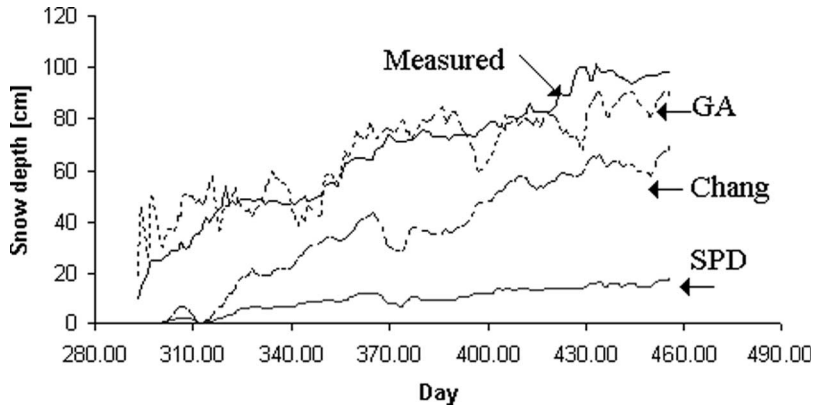

Fig. 6. GA-retrieved (continuous line) and WMO-measured (dotted line) snow depth during the season 2003–2004 at Bajkit, Siberia. The retrieved snow-depth values are smoothed by averaging five-day values.

of fractional volume are in good agreement with those ones measured in the field, with a maximum absolute error of 0.02 (relative percentage error less than 10%). Fig. 5 compares the retrieved and measured snow depths. For values of snow depth lower than 0.8 m [first three days of intensive operation period (IOP3)], the results obtained with the GA are in good agreement with the experimental data (maximum percentage error 12.6%). The error between measured and retrieved snow depth values of snow depth increases (reaching a peak of about 40%), as snow depth increases. This suggests that a threshold exists around 0.7–0.8 m of snow depth, above which the GA depth retrieval fails. These results are consistent with those reported in the literature (i.e., [2], [5], and [8]), where a threshold exists for the retrieval of snow water equivalent (SWE) and snow depth. The average threshold value for SWE is around 150 mm and for snow depth around 60–80 cm. During the observation period, high values of snow depth were present beginning February 21, corresponding to SWE values between 155 and 250 mm, when the retrieval of snow depth fails. Another factor that could be responsible for the error between measured and retrieved snow depth value is the occurrence of new snow during the period of observation. This fresh snow was characterized by small particles (0.05 mm) and very low density (lower than or comparable to 90 kg/m^3). As a consequence, the measured height of the snowpack increased, but the effect on the recorded microwave radiation was very small, due to the low sensitivity of the 19- and 37-GHz brightness temperatures to this type of snow. Stratification effects, not considered by the electromagnetic model, may also influence the performance. The comparison between GA-retrieved mean particle size (diameters) and the average values of ice-crystal size shows a minimum and maximum error of, respectively, 0.1 and 0.44 mm. The values retrieved with the GA are generally smaller than the measured ones as the DMRT tends to underestimate the mean particle size [26]. The values retrieved by means of the DMRT model (through the GA) represent the mode of a probability density function describing the particle sizes distribution where reference values of measured particles are obtained by averaging measurements carried out on particles with different shapes. This high accuracy of the matching between retrieved and measured particle size cannot be generalized and further studies are required to provide a convincing justification to the obtained results.

AMSR-E Brightness Temperatures: The GA-based technique is applied to brightness temperatures at 18.7 and 36.5 GHz recorded between October 2003 and May 2004 by the AMSR-E flying onboard the Aqua satellite. The test area is located in Siberia, Russian Federation (Bajkit, 96.36° E, 61.66° N) and it is mainly characterized by Taiga and Tundra forest. The mean annual temperature and snow depth are, respectively, -6 °C and 58 cm. The forest cover fraction for the pixel of interest is 0.35 (at 25-km resolution), and it is obtained from the moderate resolution imaging spectroradiometer (MODIS) product developed at the University of Maryland (http://modis.umiacs.umd.edu/). The GA algorithm accounts for the cover fraction by assuming that the radiation measured by the radiometer is a linear combination of forested and nonforested areas. The procedure adopted for the retrieval of snow parameters is the same as that proposed in the previous section.

Fig. 6 shows the comparison between the snow depth retrieved by using the GA-based technique (continuous line) and the values of snow depth measured by a World Meteorological Organization (WMO) station (# 238910) located close to the center of the antenna footprint (dotted line). The plotted snow depth is obtained by averaging five-day values. Obtained results show an average error of 8.29 cm, suggesting that the GA-based technique can be successfully applied for the retrieval of snow depth from satellite brightness temperatures at large scale. As a reference, in the figure, we also report the snow depth retrieved from the AMSR-E brightness temperatures by using Al Chang's algorithm for forested area [3] and the spectral polarization difference (SPD) algorithm [1]. We observe that both Chang's and the SPD algorithms provide snow-depth values lower than the measured ones with the GA technique providing best matching between retrieved and simulated brightness temperatures. The SPD algorithm does not account for the forest-cover fraction and this is the main reason why the algorithm is underestimating considerably snow depth. The Chang algorithm is a static algorithm, meaning that it assumes that mean grain size does not change along the season where the GA-based technique is a dynamic one. Fig. 7 shows the comparison between the brightness temperatures acquired by the AMSR-E (continuous black line) and those ones obtained by running the DMRT model with the parameters retrieved by the GA (dotted line). In the figure, the differences between the fitted and measured brightness temperatures are also plotted (right axes, gray line).

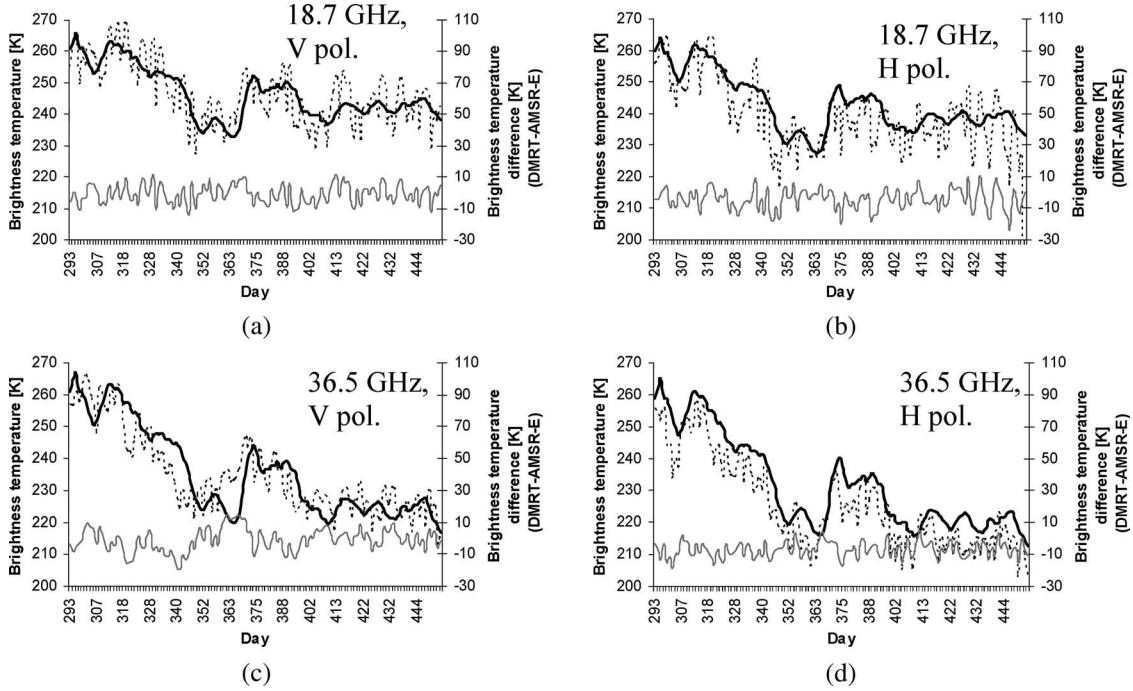

Fig. 7. Comparison between AMSR-E measured (continuous black line) and fitted (dotted line) brightness temperatures at 18.7 and 36.5 GHz, vertical and horizontal polarizations (left axes). The differences between the fitted and measured brightness temperatures are also plotted (right axes, gray line).

Unfortunately, we have no ground measurements of the other snow parameters. However, we compare the air/snow temperature trend retrieved by means of GA with the snow temperature measured by the WMO station. Results are reported in Fig. 8, where the continuous line represents the GA-retrieved snow temperature and the dotted line represents measured air temperature. The percentage error between retrieved and measured temperatures is also reported (right axis). Although discrepancies occur between the values retrieved with the two techniques, the general trend of the two sets of snow temperatures is well comparable. The obtained results are encouraging because they show that the GA-based technique is able to provide a solution whose trend is physically reasonable.

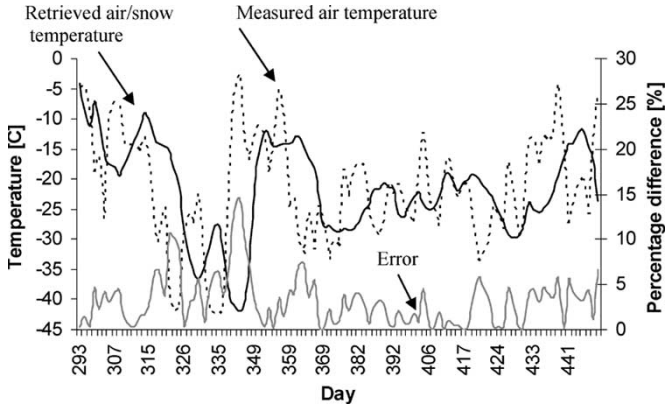

Fig. 8. GA-retrieved snow temperature averaged over five days (continuous line) and measured air temperature (dotted line). The relative percentage difference between retrieved and measured temperatures is also reported.

V. Conclusion and Future Work

A technique based on GAs and dense-medium theory has been proposed for the retrieval of dry-snow parameters from microwave brightness temperatures (18.7 and 36.5 GHz). The technique has been applied to both simulated and measured brightness temperatures.

Results obtained in the case of simulated brightness temperatures show that the proposed technique is able to retrieve the snow parameters very satisfactorily. In the cases of both noisy and noise-free simulated brightness temperatures, good results have been achieved for all considered configurations of GA parameters. In general, the snow parameter retrieved with the lowest error is mean particle size. The retrieval of fractional volume is performed with an error higher than that in the case of mean-grain-size retrieval but lower than that of snow-depth retrieval. The inversion of noisy simulated brightness temperatures has also demonstrated that the number of elements in the initial population becomes an important factor for the retrieval of snow depth.

The inversion algorithm has been applied to the brightness temperatures measured during the IOP3 period (February 19–25, 2003) of the NASA CLPX. Mean particle size and snow fractional volume have been retrieved with good accuracy for all considered dates, with a maximum relative percentage error around 10%. In the case of snow depth, for high values of snow depth, the performance of the algorithm deteriorates, reaching a relative percentage error of 40%. The existence of a threshold value for the snow-depth retrieval that is related to the microwave penetration depth at 19 and 37 GHz and the presence of new fresh snow, together with the assumption on the fixed snow and soil parameters, are among the reasons for the deterioration of the algorithm performance.

The technique has been also applied to brightness temperatures collected between October 2003 and May 2004 by AMSR-E over an area located in Siberia, Russia. The retrieved snow depth is in good agreement with the values measured

on the ground by a WMO station, suggesting that the GA-based proposed technique can represent a valid tool for the retrieval of snow depth at large scale. No ground measurement was available for the remaining parameters, making impossible the evaluation of the performance of the retrieval technique. However, in the case of air/snow temperature, good agreement has been found between the values retrieved with the GA-based technique and air temperature recorded by the WMO station.

Future work includes the evaluation of the technique to other areas and its application to wet snow.

REFERENCES

[1] J. Aschbacher, "Land surface studies and atmospheric effects by satellite microwave radiometry," Ph.D. dissertation, Institute for Meteorology and Geophysics, Univ. Innsbruck, Innsbruck, Austria, 1989.

[2] A. T. C. Chang, J. L. Foster, and D. K. Hall, "Nimbus 7 SM derived global snow cover patterns," *Ann. Glaciol.*, vol. 9, pp. 39–44, 1989.

[3] J. Foster, A. Chang, and D. Hall, "Comparison of snow mass estimates from a prototype passive microwave snow algorithm, a revised algorithm and a snow depth climatology," *Remote Sens. Environ.*, vol. 62, no. 2, pp. 132–142, Nov. 1997.

[4] R. Kelly, A. T. Chang, L. Tsang, and J. L. Foster, "A prototype AMSR-E global snow area and snow depth algorithm," *IEEE Trans. Geosci. Remote Sens.*, vol. 41, no. 2, pp. 230–242, Feb. 2003.

[5] J. T. Pulliainen, J. Grandell, and M. Hallikainen, "HUT snow emission model and its applicability to snow water equivalent retrieval," *IEEE Trans. Geosci. Remote Sens.*, vol. 37, no. 3, pp. 1378–1390, May 1999.

[6] J. Pulliainen and M. Hallikainen, "Retrieval of regional snow water equivalent from space-borne passive microwave observations," *Remote Sens. Environ.*, vol. 75, no. 1, pp. 76–85, Jan. 2001.

[7] D. T. Davis, Z. Chen, L. Tsang, J. N. Hwang, and A. T. C. Chang, "Retrieval of snow parameters by iterative inversion of a neural network," *IEEE Trans. Geosci. Remote Sens.*, vol. 31, no. 4, pp. 842–851, Jul. 1993.

[8] M. Tedesco, J. Pulliainen, P. Pampaloni, and M. Hallikainen, "Artificial neural network based techniques for the retrieval of SWE and snow depth from SSM/I data," *Remote Sens. Environ.*, vol. 90, no. 1, pp. 76–85, Mar. 2004.

[9] J. A. Nelder and R. Mead, "A simplex method for function minimization," *Comput. J.*, vol. 7, no. 4, pp. 308–313, 1965.

[10] T. Graf, T. Koike, H. Fujii, M. Brodzik, and R. Armstrong, *CLPX-Ground: Ground Based Passive Microwave Radiometer (GBMR-7) Data*. Boulder, CO: National Snow and Ice Data Center, 2003. Digital Media.

[11] M. Tedesco, E. J. Kim, D. Cline, T. Graf, T. Koike, R. Armstrong, M. Brodzik, and J. Hardy, "Dense media modelling of local-scale snowpacks during the cold land processes experiment-1: A sensitivity analysis," in *Proc. MicroRad Spec. Meeting*, Rome, Italy, Feb. 24–27, 2004, pp. 1345–1346.

[12] ——, "Analysis and modelling of cold land process experiment-1 ground-based data acquired during the third intensive observation period (IOP3)," *Hydrological Processes*, vol. 20, pp. 657–672, 2006.

[13] I. Rechenberg, *Cybernetic Solution Path of an Experimental Problem,* Royal Aircraft Establishment. Farnborough, U.K., Library Translation 1122, 1965.

[14] ——, "Evolutionsstrategie: Optimierung Technischer Systeme nach Prinzipien der Biologischen Evolution," M.S. thesis, Dept. Process Eng., Tech. Univ. Berlin, Berlin, Germany, 1971.

[15] ——, *Evolutionsstrategie: Optimierung Technischer Systeme nach Prinzipien der Biologischen Evolution*. Stuttgart, Germany: Frommann-Holzboog Verlag, 1973.

[16] J. Holland, *Adaptation in Natural and Artificial Systems*. Cambridge, MA: MIT Press, 1992.

[17] L. Tsang, J. A. Kong, and R. T. Shin, *Theory of Microwave Remote Sensing*. New York: Wiley, 1985.

[18] Y. Q. Jin, *Electromagnetic Scattering Modelling for Quantitative Remote Sensing*. Singapore: World Scientific, 1993.

[19] M. Tedesco, "Microwave remote sensing of snow," Ph.D. dissertation, Inst. Appl. Phys. "Carrara", Firenze, Italy, 2003.

[20] Z. Michalewicz, *Genetic Algorithms + Data Structures = Evolution Programs*. AI Series. New York: Springer-Verlag, 1994.

[21] J. Antonisse, "A new interpretation of schema notation that overturns the binary encoding constraint," in *Proc. 3rd Int. Conf. Genetic Algorithms*, J. D. Schaffer, Ed, San Mateo, CA, 1989, pp. 86–91.

[22] N. J. Radcliffe, "Nonlinear genetic representations," in *Parallel Problem Solving From Nature 2*, R. Männer and B. Manderick, Eds. Amsterdam, The Netherlands: Elsevier, 1992, pp. 259–268.

[23] C. Houck, J. Joines, and M. Kay, "A genetic algorithm for function optimization: A Matlab implementation," North Carolina State Univ., Charlotte, NCSU-IE TR 95-09, 1995.

[24] G. Hufford, "A model for the complex permittivity of ice at frequencies below 1 THz," *Int. J. Infrared Millim. Waves*, vol. 12, no. 7, pp. 677–682, Jul. 1991.

[25] J. Hardy, J. Pomeroy, T. Link, D. Marks, D. Cline, K. Elder, and R. Davis, *Snow Measurements at the CLPX Local Scale Observation Site (LSOS)*, M. Parsons and M. J. Brodzik, Eds. Boulder, CO: National Snow and Ice Data Center, 2003. Digital Media.

[26] M. Tedesco and E. J. Kim, "Intercomparison of electromagnetic models for passive microwave remote sensing of snow," *IEEE Trans. Geosci. Remote Sens.*, vol. 44, no. 10, Oct. 2006. to be published.

Marco Tedesco (M'00) received the laurea degree in electronic engineering from the University of Napoli "Federico II," Naples, Italy, in 1999, and the Ph.D. degree from the Institute of Applied Physics "Carrara," Firenze, Italy, in 2003, with the thesis titled "Microwave Remote Sensing of Snow."

He was a Visiting Student at the Chinese Academy of Science, Beijing, the Fudan University, Shanghai, China, and the Space Laboratory of the Helsinki University of Technology. Since 2003, he has been with the Goddard Earth Science Technology Department of the University of Maryland, Baltimore County, and with the National Aeronautics and Space Administration Goddard Space Flight Center, Hydrospheric and Biospheric Sciences Laboratory, Greenbelt, MD. He also collaborated with the Group of Interaction between Electromagnetic Fields and Matter of the Institute of Research on Electromagnetic Waves publishing several peer-reviewed papers on microwave measurement techniques. His research interests include remote sensing of snow, ice, and soil; data fusion and assimilation; spatial behavior of geophysical parameters and remote sensing data; retrieval of snow impurities; merging hydrological and electromagnetic models; and measurement of dielectric properties of natural media.

Dr. Tedesco was the recipient of the NASA Outstanding PostDoc/Research Associate Peer Award in August 2005, and in October of the same year, he received the Young Scientist URSI Award. He serves as a Reviewer for several journals and is Member of IEEE Geoscience and Remote Sensing Society, the American Geophysical Union Society, the Technical Committee of Frequency Allocation in Remote Sensing, and the National Geographic Society.

Edward J. Kim (S'86–M'97–SM'05) received the S.B. and S.M. degrees in electrical engineering from the Massachusetts Institute of Technology, Cambridge. He received the joint Ph.D. degrees with the Departments of Electrical Engineering and Atmospheric Sciences at the University of Michigan, Ann Arbor, in 1998.

Since 1992, he has been involved in remote-sensing field experiments related to the cryosphere, land, atmosphere, and oceans. Since 1999, he has been at National Aeronautics and Space Administration Goddard Space Flight Center in the Hydrospheric and Biospheric Sciences Laboratory, Greenbelt, MD, developing and applying Earth remote-sensing techniques, particularly for the cryosphere. Recently, he has spearheaded efforts at Goddard to support a satellite proposal from the cold land processes community. He is Principal Investigator for several NASA airborne and ground-based radiometers. He also serves the U.S. National Polar-orbiting Operational Environmental Satellite System program as Senior Instrument Scientist for the Advanced Technology Microwave Sounder microwave atmospheric sounder, and as a Member of the Microwave Operational Algorithm Team. His interests include the modeling of snow, ice, soil, and vegetation; radiative transfer theory; and the development of new observational tools.

Dr. Kim was selected for a National Research Council Research Associateship, in 1997. In 1998, he was awarded second prize in the International Geoscience and Remote Sensing Symposium student paper competition.